Influence of soil-structure interaction on structural behaviour of integral bridge piers

DAMIEN DREIER

Structural Concrete Laboratory (IS-Béton),
Ecole Polytechnique Fédérale de Lausanne (EPFL)
CH-1015 Lausanne, Switzerland
damien.dreier@epfl.ch

Abstract

Over the past decades, an increasing number of integral bridges have been built. This is justified by the various advantages of integral bridges in comparison with standard bridges equipped with expansion joints and bearings. In particular, integral bridges require less maintenance because they do not have mechanical elements and they have an enhanced structural performance because of the frame action and contribution to the stiffness of the embankment at the abutments. However, the structural behaviour of integral bridges is at present not fully understood. This is due to the complexity of the complete system, which must be studied considering the soil-structure interaction.

Piers monolithically connected to the bridge deck undergo large displacements caused by creep, shrinkage and temperature effects. This paper investigates the structural behaviour of piers of integral bridges considering the interaction between the foundations of the piers and the surrounding soil. The cracking limit state is investigated considering short-term imposed strains in the bridge deck as a function of the maximal horizontal displacement allowable at the top of the pier.

1. Introduction

Over the past decades, an increasing number of integral bridges have been built, benefiting from the various advantages related to the elimination of expansion joints and bearings (Figure 1). This allows maintenance cost to be reduced and improve the structural performance because of the frame action and of the contribution to the stiffness of the embankment at the abutments. However, due to the fact that the structure is monolithic, the soil-structure interaction needs to be taken into account in analysing the whole system behaviour (bridge, soil foundation and embankment). Over the last decades, several researchers have been studying the influence of soil-structure interaction on the behaviour of integral bridges.[1,2,3,4]

The interaction between soil and structure has been investigated since the eighteenth century.[5] The first research studied the lateral pressure behind the walls.[6] More recently, various studies have been conducted on the influence of the pressure of soil on stiff and flexible culverts[5] and on cut-and-cover tunnels.[7,8] These studies showed the complexity of soil-structure interaction and the necessity to take into account the properties of the soil together with the geometry and stiffness of the structure to determine the distribution of pressure on the structure and to assess its structural behaviour.

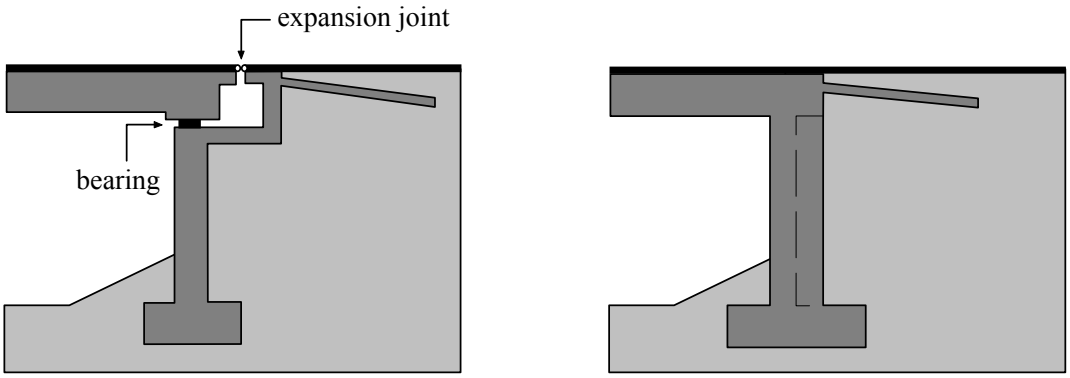

(a) (b)

Figure 1: Standard and integral bridge abutment details
(a) Standard bridge abutment; (b) Integral bridge abutment

The most important problems for the integral bridges are the settlements near the abutment or the transition slab and cracking of structural elements such as the bridge deck, abutment wall, piers and transition slab.[9] Disorders may result from the imposed deformation of the bridge deck caused by creep (ε_{cr}), shrinkage (ε_{sh}) and temperature variations ($\varepsilon_{\Delta T}$). Short piers rigidly connected to the deck and located far from the fix point (a point at the deck exhibiting no longitudinal displacement) can be subjected to a large imposed displacement at its top that can cause significant cracking (Figure 2). These cracks can be unacceptable for the serviceability limit state (SLS).

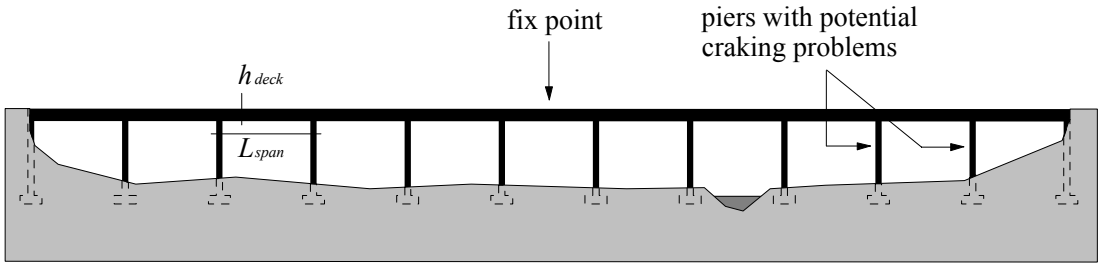

Figure 2: Position of the studied piers

This paper investigates the structural behaviour of bridge piers considering the interaction between the foundations of piers and the surrounding soil. The cracking limit state is investigated as a function of the maximal horizontal displacement allowable on top of the pier (u_{adm}). The horizontal displacement (u) can be calculated from the imposed strains in the bridge deck ($\varepsilon_{imp} = \varepsilon_{cr} + \varepsilon_{sh} + \varepsilon_{\Delta T}$) and the distance between the pier and the fix point ($L_{p\text{-}p,fix}$). This value ($u = \varepsilon_{imp} L_{p\text{-}p,fix}$) should remain smaller than the value acceptable due to cracking (u_{adm}).

2. Theoretical approach

Cracking of the pier is evaluated using a numerical model that takes into account the behaviour of the foundation and the pier. The bridge deck is considered to be infinitely stiff so that the relative rotation between the top end of the pier and the deck is neglected.

In a first step, the behaviour of the foundation and the pier are studied separately. The behaviour of the foundation is characterized by a moment-rotation (m-θ) relationship and a shear force-sliding (v-δ_u) relationship (Figure 4(a)), whereas the pier behaviour is characterized by a moment curvature (m-κ) relationship.

In a second step, the whole system presented in Figure 3 is modelled including the equilibrium of internal forces and the kinematics compatibility between the elements studied in the first step.

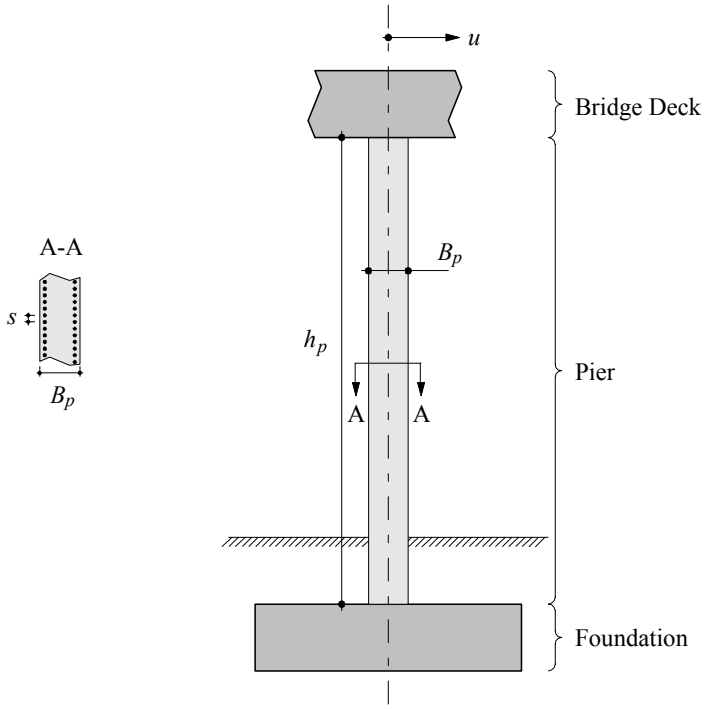

Figure 3: Horizontal of the cross-section investigated system

3. Modelling of the foundation

In this step, the foundation is modelled without considering its interaction with the rest of the pier. The case is illustrated in Figure 4.

The foundation is assumed infinitely stiff, so there is no structural deformation. The foundation soil is considered granular, cohesionless and without first nor secondary creep.

The main parameters of the shallow/footing foundation geometry are: the depth h_{soil} of soil, the width B_f and the thickness h_f of foundation. The length of the foundation is assumed sufficient so that its modelling can be performed in considering a plane state of deformation. The axial force n, the shear force v and the bending moment m are given in per linear meter.

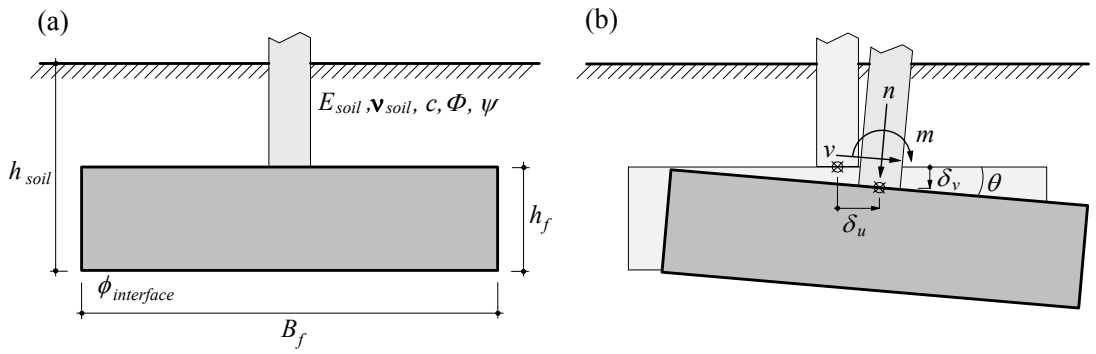

Figure 4: Modelling of the foundation
(a) Soil and foundation parameters; (b) forces and foundation displacements

An elastic-plastic soil behaviour according to a Mohr-Coulomb failure criterion is assumed. The parameters describing the elastic behaviour of soil are the modulus of elasticity of soil (E_{soil}) and the Poisson's ratio (ν_{soil}). The parameters describing the Mohr-Coulomb criterion are: the cohesion (c), the frictional angle (Φ) and the dilatancy angle ($\psi = 2/3\ \Phi$). Finally, one parameter is associated with the roughness of the interface between the foundation and the soil ($\phi_{interface}$).

The assumed parameters for the soil are summarized in Table 1 and the geometry of foundation in Table 2. All simulations were performed using ZSoil[10], a finite element model specialized in the modelling of the behaviour of soil.

Table 1: Assumed soil parameters

	E_{soil} [MPa]	ν_{soil} [-]	c [kPa]	Φ [°]	Ψ [°]
Min,value	50	0.25	1	30	20
Mean value	100	0.32	1	35	23
Max,value	200	0.45	1	40	27

Table 2: Geometry of the foundation

	h_{soil} [m]	B_f [m]	h_f [m]	$\phi_{interface}$ [°]
Min,value	1	2	0.5	0
Mean value	2	4	1	25
Max,value	3	6	1.5	35

3.1. Failure mode and serviceability limit state (SLS) behaviour of soil foundation

Three main mechanisms, related to n, v or m, can lead to soil failure. The first mechanism, associated with n, is the punching of the soil. The second mechanism, associated with v, is a translation mechanism (sliding of the foundation) with the activation of a passive zone in front of the foundation and an active zone behind the foundation. The last mechanism, associated with m, is a global rotation with active and passive zones around the foundation. In

the parametric analysis, all modelled foundations have reached their ultimate capacity with a translation mechanism.

The foundation response at SLS can be described by two diagrams. The first expresses the rotation as a function of the applied moment (Figure 5) and the second expresses the translation as a function of the applied shear force (Figure 6).

Bridges considered in this study correspond to slab bridge with spans L_{span} in the range of 20 to 25 m and a deck thickness h_{deck} to have a bridge slenderness L_{span}/h_{deck} in the range of 20 to 30. Consequently, the normal force n at the top of piers is considered equal to 500 kN/m (per m of width). The dimensions of the foundations are determined to avoid unacceptable settlements.

3.2. Influence of soil and structure parameters

The influence on m-θ and on v-δ_u of the soil and the structure parameters is shown in Figures 5 and 6. If not is indicated otherwise, the curves are obtained using the mean value of the Tables 1 and 2.

Some parameters influence more significantly the foundation response at the serviceability limit state (SLS) and others govern ultimate limit state (ULS). The modelling has shown that the most important parameters influencing the rotational and transversal rigidity at the SLS are the soil modulus E_{soil}, the depth of the soil foundation h_{soil} and the width of foundation B_f.

Based on the results shown in Figure 5, it can be noted that the rotational rigidity is approximately linearly proportional to E_{soil}, proportional to the square root of h_{soil} and proportional to the square of B_f. The modelled effect of E_{soil} and B_f are in accordance with the analytic results obtained with a formulation based on the elastic theory (Eq. 1).[11]

$$k_f = \frac{B_f^2 \, \pi \, E_{soil}}{16(1-\nu_{soil}^2)} \text{ [MNm/m]} \qquad (1)$$

However, this analytical formulation does not take into account the depth of the foundation h_{soil}, which shows a significant influence according to the FE results. These parameters have an important effect on the translational behaviour too. Contrary to the rotational behaviour, it is however more difficult to find a direct relationship between the variations of parameters and the translational stiffness (Figure 6).

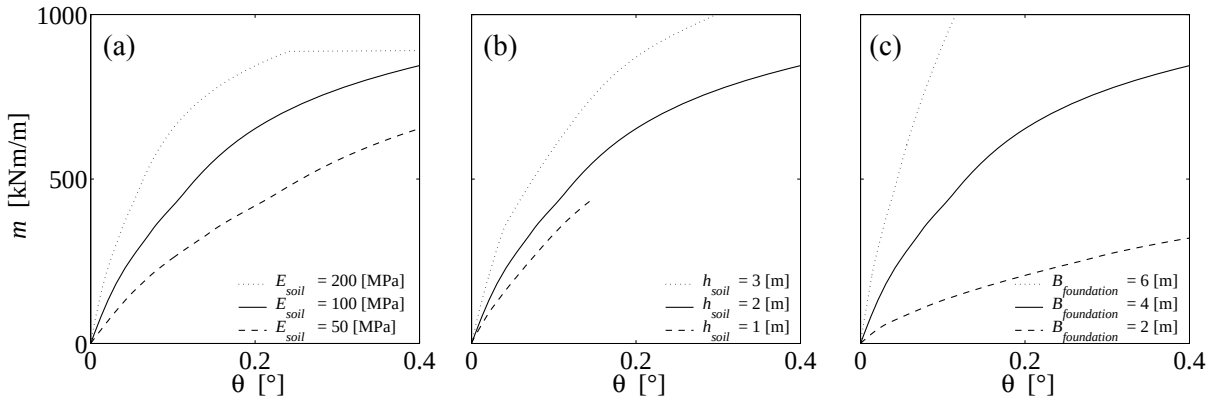

Figure 5: Moment-rotation curves for various condition
(a) Effect of E_{soil}; (b) Effect of h_{soil} ; (c) Effect of $B_{foundation}$

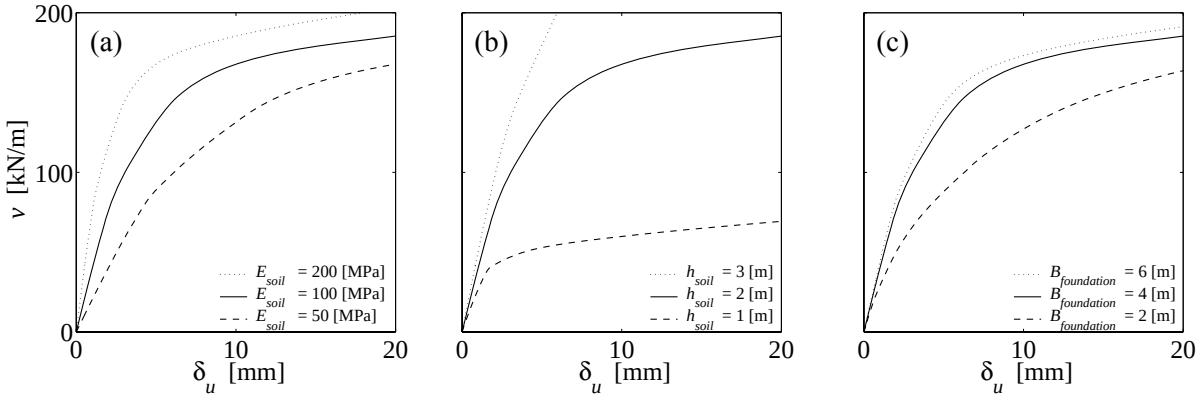

Figure 6: Shear force-translation for various condition
(a) Effect of E_{soil}; (b) Effect of h_{soil} ; (c) Effect of $B_{foundation}$

4. Modelling of the piers

A numerical model was developed to simulate the column behaviour. The implementation was done with the software Matlab.

It is assumed that the behaviour can be described with enough precision in considering only the flexural behaviour of the column. So the curvature is directly proportional to the moment (2) and the transverse displacement can be directly evaluated by the double integration of the curvature (3).

$$\chi(x) = f\big(m(x)\big) \tag{2}$$

$$\chi(x) = \frac{d^2u(x)}{dx^2} \tag{3}$$

The main difficulty of this analysis is the determination of m-χ relationship. Using the hypotheses that plane sections remain plane and the condition of static equilibrium, the m-χ relationship taken into account the effect of cracking can be obtained for any section and reinforcement distribution. Moreover, this relationship depends on concrete time dependent behaviour. So a time-dependent analysis based on the aging coefficient method[12] was performed considering the effect of shrinkage and nonlinear creep[13]:

$$\Delta\varepsilon_{cc} = \varepsilon_c(t_0)\cdot\varphi\left(t,t_o,\frac{\sigma_c}{f_c}\right) = \varepsilon_c(t_o)\cdot\varphi_{lin}(t,t_0)\cdot\eta\left(\frac{\sigma_c}{f_c}\right) \text{ and } \eta\left(\frac{\sigma_c}{f_c}\right) = 1+2\cdot\left(\frac{\sigma_c}{f_c}\right)^4 \tag{4}$$

4.1. Comparison with experimental data

Figure 7 presents the comparison between experimental results obtained by Dal Busco et al.[14] at EPFL and the results from the numerical simulation developed in this study. The predictions of the numerical results show a good accordance with the test data (Figure 7(c) to (g)): the average ratio AVG of w_{test}/w_{model} at t_0 and at t_∞ are 1.06 and 0.93 respectively and the corresponding coefficients of variation CoV are 11 and 12 %. Based on this, the proposed approach can be used with confidence to model the structural response of columns.

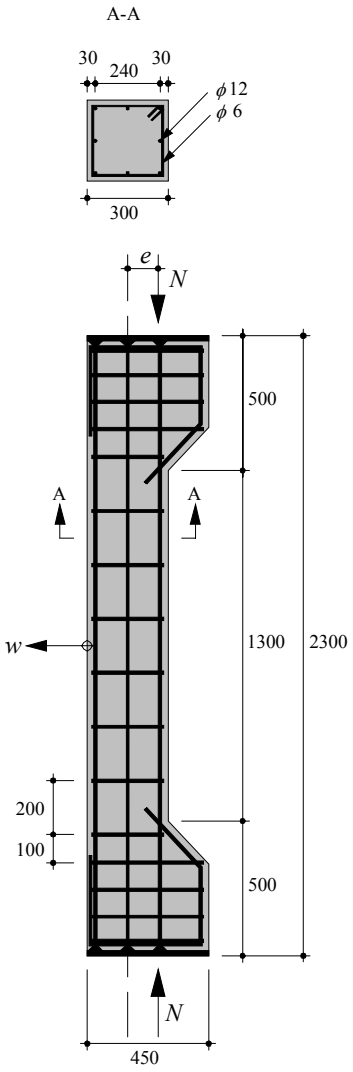

(a)

Specimen	A1	A2	A3	A4	A5	A6	A7
N [kN]	-267	-267	-267	-515	-515	-515	-787
e [m]	0.092	0.145	0.198	0.072	0.093	0.113	0.065

(b)

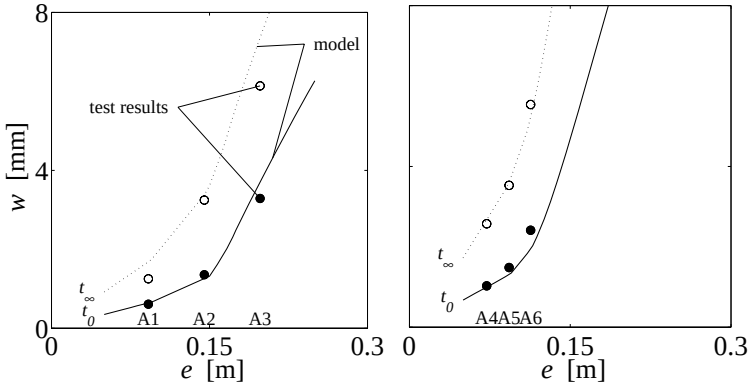

(c)

(d)

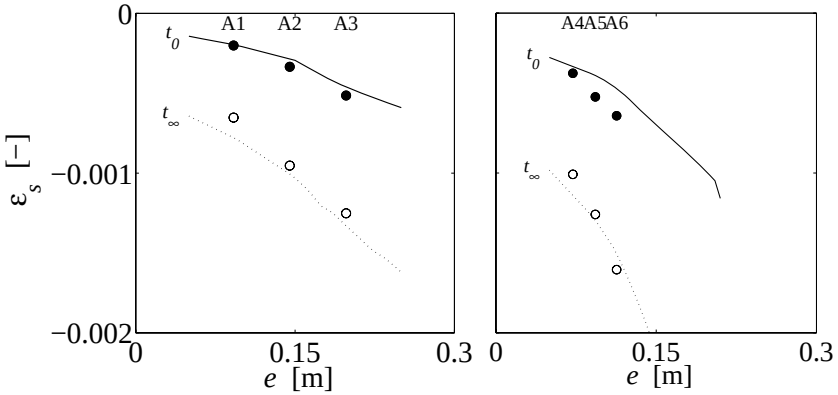

(e) (f)

Specimen	A1	A2	A3	A4	A5	A6	A7	AVG	CoV [%]
w_{test}/w_{model} at t_0	0.95	1.07	0.89	1.03	1.15	1.25	1.08	1.06	11
w_{test}/w_{model} at t_∞	0.74	0.96	0.83	0.96	0.98	1.07	0.96	0.93	12

(g)

Figure 7: Comparison between the results of the numerical simulation and the test data[14] (a) Geometry of specimens [mm]; (b) Properties of specimens (fix parameters: f_c = 38.9 [MPa], f_{ct} =3 [MPa], $E_{c,o}$ =34'900 [MPa], φ_{lin} = 1.76 [-]and ε_{sh} = -0.32 [‰]); (c) w for N/A = 0.08 f_c [MPa]; (d) w for N/A = 0.15 f_c [MPa]; (e) ε_s for N/A = 0.08 f_c [MPa]; (f) ε_s for N/A = 0.15 f_c [MPa]; (g) Comparison between test results and numerical simulation (AVG: average ratio and CoV: coefficient of variation)

5. Influence of the soil-structure interaction on the pier behaviour

In this section, the influence of the foundation stiffness k_f at SLS and the pier response on the allowable imposed displacement u_{adm} at the top of the pier is investigated. The foundation stifness k_f can be characterized by the elastic rigidity of an infinitely stiff and long foundation (Eq. (1)). In addition, the allowable displacement has been normalized ($u_{adm}B_p/h_p^2$)

The investigated system is the structure presented in Figure 3 and includes the previously studied elements. In this case, the v-δ_u relationship is neglected and the depth of soil is considered constant h_{soil} = 2 m. Moreover, the concrete characteristics are only considered under short-time loading, so the concrete elastic modulus E_c = 30'000 MPa remains constant as well as its design compressive strength f_{cd} = 30 MPa and its tensile strength f_{ctd} = 3 MPa. The assumed characteristics of the reinforcing bars are this elastic modulus E_s = 205'000 MPa and the design yield strength f_{sd} = 435 MPa. The normal stress n and the soil and foundation parameters are considering according to the paragraph on foundation modelling.

Figure 8 shows the effect of k_f for different reinforcement ratio $\rho = A_s/A$, where A_s is the cross-section area of reinforced bar and A the cross-section of the pier, on u_{adm} for the more severe level of compliance on the cracking limit state according to the Swiss code for structural concrete.[15] In this case, the allowable imposed displacement u_{adm} leads to a crack opening of approximately of 0.1 mm. According to this code, for a spacing of the longitudinal bars s = 100 mm, an admissible stress $\sigma_{s,adm}$ = 300 MPa is obtained.

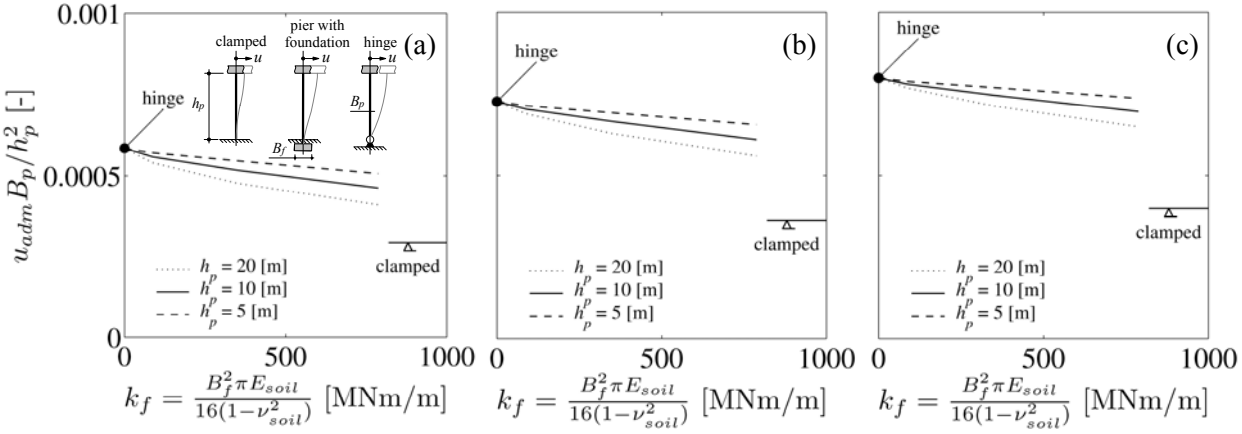

Figure 8: Effect of the foundation stifness k_f and the reinforcement ratio ρ on the allowable displacement u_{adm} at the top of the pier for a allowable stress $\sigma_{s,adm}$ = 300 [MPa] in the reinforcement and a pier thickness B_p = 0.5 [m] and comparasion with a base hinge and base claped pier
(a) ρ = 1 [%]; (b) ρ = 2 [%]; (c) ρ = 3 [%]

Figure 8 shows the influence of the stiffness of the foundation k_f on the allowable imposed displacement u_{adm}. If k_f is low (soft soil and/or short width foundation) a situation for the pier similar to having a hinge results. If the soil and the width of the foundation are intermediate, the pier is partly clamped. Finally, if the foundation stiffness is very large (hard soil/rock or very wide foundation), the statical system of the pier becomes clamped-clamped reducing consequently the value of u_{adm}. It can be seen that the consideration of the stiffness of the foundation is significant with reference to the allowable cracking at SLS.

Figure 8 also shows that the height of the pier is an important parameter in the consideration of the normalized allowable imposed displacement $u_{adm}B_p/h_p^2$. Indeed, taller a pier is less sensitive to the SLS crack limitation because the ratio between the rigidity of pier and the foundation is smaller than for a short pier.

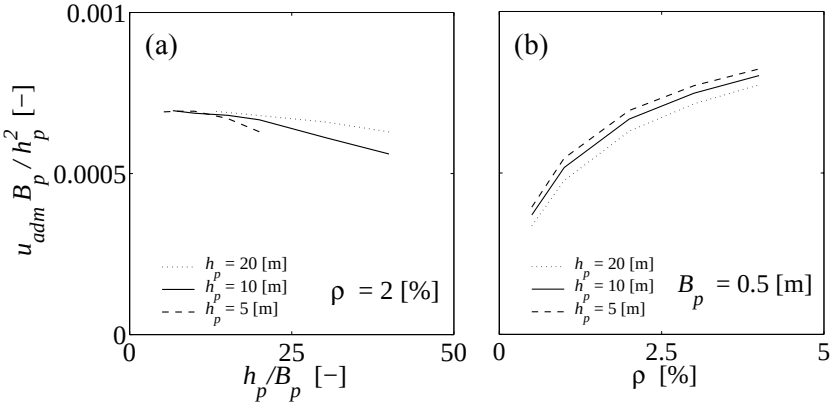

Figure 9: Parameter influence on u_{adm} for σ_{adm} = 300 [MPa] and k_f = 350 [MNm/m]
(a) Effect of slenderness h_p/B_p; (b) effect of renforcement ratio ρ

Figure 9(a) shows that the slenderness h_p/B_p is not significant in the range of standard construction (h_p/B_p between 10 and 30). However, Figure 9(b) shows the significant effect of reinforcement ratio ρ on the normalized allowable displacement. Clearly, an increase of ρ increases the allowable displacement but in a less than proportional manner.

6. Conclusions

This paper investigates the importance of soil structure interaction to evaluate the allowable imposed displacement u_{adm} at the top of piers accounting for the cracking limit state. The main conclusions are:

1. The influence of the stiffness of the foundation k_f is very significant in the evaluation of u_{adm}. A low stiffness leads to a static system with a hinge at the base of the pier. On the contrary, a large stiffness leads to a static system clamped at the base;
2. The pier height h_p is also significant, a high pier is less sensitive to imposed displacement that a short pier;
3. The reinforcement ratio ρ is also significant but the increase in u_{adm} is less then linearly proportional to ρ.

6.1. Further work

This study is in progress at the current time. Some assumptions need still to be improved. The influence of the structural stiffness of the foundation, of second order effects, of the time-dependent behaviour of concrete, of soil compaction with cyclic rotation of the foundation[16] and the effect of v-δ_u and n need to be investigated.

References

[1] **Pritchard B.** *, Continuous and Integral Bridges*, E & FN SPON, **1994**.

[2] **Pötzl M.** *, Robuste Brücken*, Vieweg, 288pp, Braunschweig, Germany, **1996**.

[3] **England G. L., Tsang N. C. M., Bush D. I.** *, Integral bridges a fundamental approach to the time-temperature loading problem*, Thomas Telford, **2000**.

[4] **FHWA** *, Integral Abutment and Jointless Bridges*, The 2005 - FHWA Conference, Baltimore, USA, March, **2005**.

[5] **Linger D. A.** *, Historical development of the soil-structure interaction problem*, Soil-structure interaction: a symposium, Highway Research Board n°413, pp. 5-12, USA, **1972**.

[6] **Heyman J.** *, Coulomb's memoir on statics, an essay in the history of civil engineering*, Cambridge University Press, Cambridge, England, **1972**.

[7] **Kovári K., Tisa A.** *, Computational Model and Charts for cut-and-cover tunnels*, Int. Ass. Bridges and Str. Eng., **1998**.

[8] **Plumey S.** *, Interaction sol-structure dans le domaine des tranchées couvertes*, Thèse EPFL, N° 3714, 299 p., Lausanne, Switzerland, January, **2007.**

[9] **Maruri R. F., Petro S. H. ,** *Integral Abutments and Jointless Bridges (IAJB) 2004 Survey Summary*, The 2005 - FHWA Conference, 12-26, Baltimore, USA, **2005.**

[10] **Zace Service SA** *, Z.Soil.PC.2003 user manual*, Elmepress, Lausanne, Switzerland, **2003.**

[11] **Bowles J. E.** *, Foundation Analysis and Design, Fifth Edition*, McGraw-Hill, 1241 pp., USA, **1997.**

[12] **Fernández Ruiz M.** , Evaluación no lineal de los efectos estructurales producidos por las deformaciones diferidas del hormigón y el acero, Universidad Politécnica de Madrid, 175p., Madrid, Spain, **2003.**

[13] **Fernández Ruiz M., Muttoni A., Gambarova P.** *, Relationship between nonlinear creep and cracking of concrete under uniaxial compression*, Journal of Advanced Concrete Technology, Vol. 5, No 3, pp. 383-393, Japan, **2007**.

[14] **Dal Busco S., Najdanovic D., Suter R.** *, Dimensionnement des colonnes de bâtiment, essais de longue durée série expérimentale A et B*, Publication IBAP, 116, Lausanne, Switzerland, December, **1986**.

[15] **SIA** *, Concrete Structures*, Swiss Society of Engineers and Architects, 90 p., Zurich, Switzerland, **2004**.

[16] **England G. L., Tsang C. M., Dunstan T., Wan R. G.** *, Drained granular material under cyclic loasding with temperature-induced soil/structure interaction*, Architectural Press, 50, 553-579, USA, 10, **1997**.